DOI: 10.18462/iir.gl2022.0103

Results from measurements of heat pump for district heating using ambient air as heat source

Svenn Ole Kjøller HANSEN*[(a)], Jonas Kjær JENSEN[(b)], Matteo DOMINATO[(c)], Lars Ove REINHOLDT[(c)], Wiebke Brix MARKUSSEN[(b)]

[(a)] DTI Danish Technological Institute
Aarhus, DK8000, Denmark, sha@teknologisk.dk
[(b)] DTU Technical University of Denmark
Kgs. Lyngby, DK2800, Denmark, jkjje@mek.dtu.dk, wb@mek.dtu.dk
[(c)] PlanEnergi
Aarhus, DK8000, Denmark, md@planenergi.dk, lr@planenergi.dk

*Corresponding author: sha@teknologisk.dk

ABSTRACT

Intensive measurements on 2 out of 20 evaporators have been made on a 6.5 MW ammonia heat pump for district heating at Brædstrup Fjernvarme Amba in Denmark as part of a project called "Optimization of large heat pumps using ambient air". The goal of the project is to optimize and develop the evaporator design and control of the heat pump in relation to frosting, defrosting, and noise. The system is af pump circulation type with evaporators of flatbed type having 8 fans each designed for direction of air flow downwards. The measurements include the weight of the evaporators, the electrical power consumption of each fan, temperatures of air entering and leaving the evaporator, refrigerant flow, and temperatures of the evaporator coils. CFD-work compared to analysis of the measurements shows recirculation of air depending on wind direction and speed. Analysis of measurements have led to development of a new defrost control for effective defrost with use of minimum energy. This paper presents interesting results and conclusions about performance and defrost from the measurements.

Keywords: Evaporator, defrost, ammonia, heat pump, ambient air, district heating

1. INTRODUCTION

The primary challenges connected to the use of ambient air as heat source for large heat pump systems for district heating are performance, frosting and defrosting as well as noise of the evaporators (Jensen et al., 2019). Factors such as weather conditions, physical placing of the evaporator, and the construction of the evaporator all have significant influence on the performance of the evaporator. Problems related to frosting and defrosting of the evaporator constitute a risk relative to operational down time and have a significant impact on the energy efficiency of the heat pump (Kristófersson et al., 2018). Neighbors and regulatory requirements set requirements for a maximum level of noise.

These challenges are dealt with in the project "Optimization of large heat pumps using ambient air" which is supported by the Danish Energy Technology Development and Demonstration Program (EUDP). The objective of the project is to develop and demonstrate new innovative solutions which address the mentioned challenges by optimizing and developing the evaporator design and control of frosting and defrosting. A part of the project consists of carrying out measurements at a 6.5 MW heat pump installation at the Danish district heating site Brædstrup Fjernvarme to map and understand exactly how the plant works – and thus to use this knowledge for the optimization and development processes.

This paper describes some of the measurements as well as the knowledge and the results which have emerged from analyzing these measurements.

2. SYSTEM DESCRIPTION

The heat pump installation at Brædstrup Fjernvarme Amba, which was installed by Innoterm A/S, is a two-stage ammonia plant of approx. 6.5 MW heat capacity with a supply temperature of 70°C water to end consumers. The installation has following main components: 2 screw compressors, 1 piston compressor, 1 intermediate cooler, 1 economizer, 6 plate heat exchangers, t2 pump separators, and 20 evaporators. Figure 1 shows the compressors and the economizer inside the building and figure 2 shows pump separators and evaporators outside next to the building. Figure 5 shows the total plant set-up with position of components both inside and outside:

Figure 1: Main components in the building for the heat pump

Figure 2: Pump separators and evaporators placed outside

The evaporators shown in figures 3 and 4 are produced and delivered by Fincoil Luve Oy. The evaporators are of the ’flatbed’ type, each with 2 individual coils with pipes of stainless steel and 8 fans and aluminum fins with a spacing of 5 mm. Each evaporator has been calculated to have a ‘cooling capacity’ of 195 kW without frosting at an air inlet temperature of -4°C, a relative humidity of 90%, an air outlet temperature at -8°C, and an evaporation temperature of -10°C as well as a circulation rate of 2 on the ammonia side.

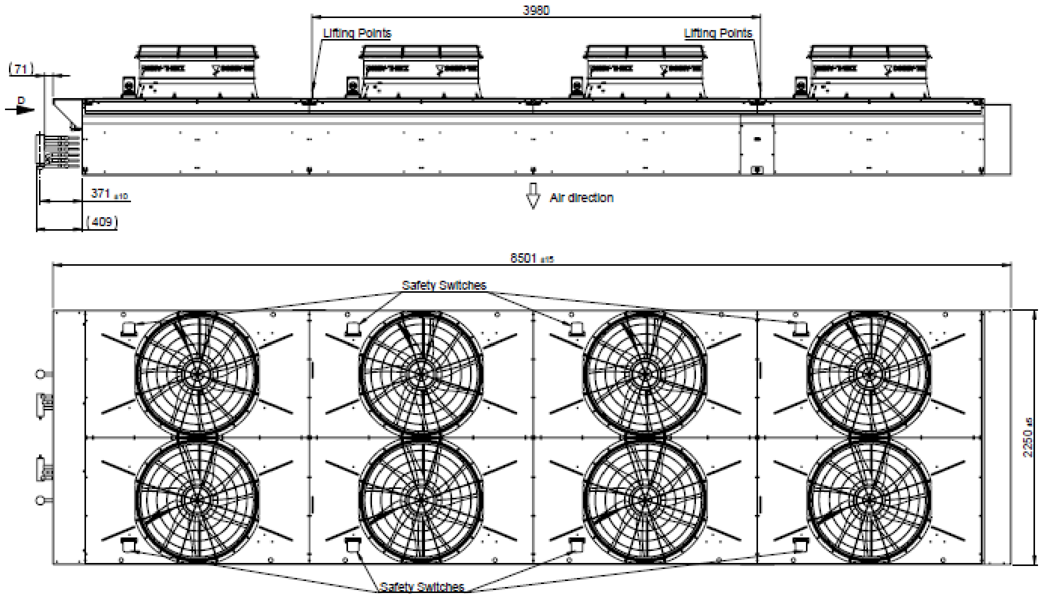

Figure 3: Drawing of the evaporator at Brædstrup Fjernvarme

Figure 4: Picture of the evaporators at Brædstrup Fjernvarme

The 20 evaporators are installed next to the machine building in a row of about 45 meters and placed on a stand, which is approx. 3 meters above ground level as shown in figure 4.

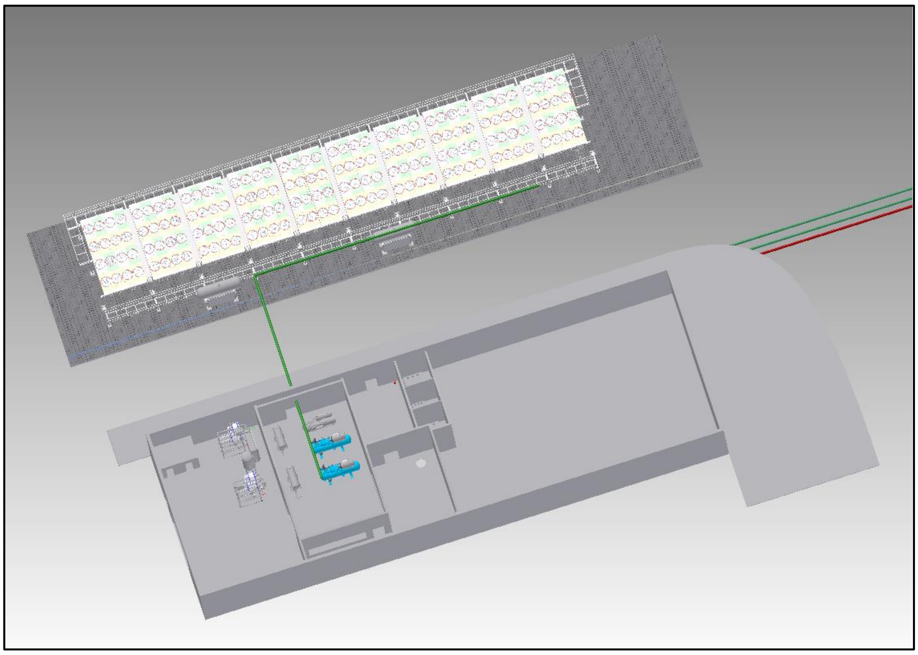

Figure 5: Set-up of evaporators and machine building at Brædstrup Fjernvarme

3. MEASUREMENTS

Extensive measurements have been made on both temporary as well as stationary equipment on 2 of the 20 evaporators. The temporary measuring equipment is established for the duration of the project by Danish Technological Institute while the stationary measuring equipment is a part of the IGSS system (Interactive Graphical SCADA System - Supervisory Control And Data Acquisition) at Brædstrup Fjernvarme. The 2 selected evaporators (#15 and #16 shown on figure 7), which are subject for the measurements, are placed next to each other, but they are not placed in the middle nor at the end of the row of evaporators as seen on figure 6.

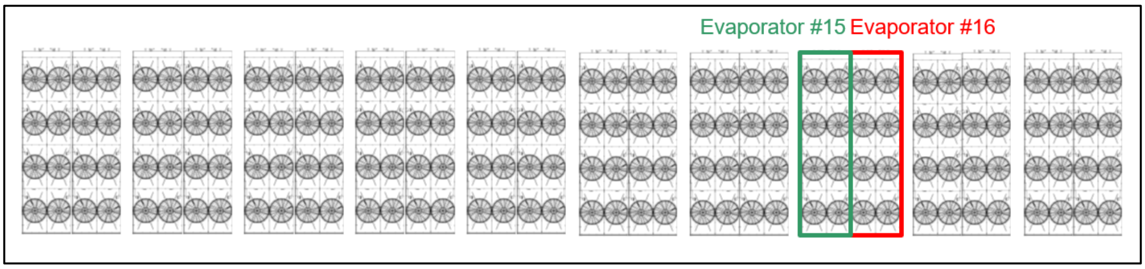

Figure 6: the 20 evaporators with position of evaporator #15 and #16 at the plant in Brædstrup

Evaporator #15 serves as 'reference' as it has the same valves and controls as eighteen of the other evaporators in the row. Evaporator #16 is an experimental and test evaporator which can be operated as the other nineteen evaporators, or it can be operated with another setup of valves and controls. From the beginning of the heat pump plant operation in January 2022, the supply of liquid to evaporator #15 has been carried out with a fixed opening degree of a regulation valve. In comparison, the supply of liquid to evaporator #16 has been controlled by an electronic regulator with a superheat setting of 1°K and a supply of liquids controlled by opening and closing of a valve using the pause/pulse method.

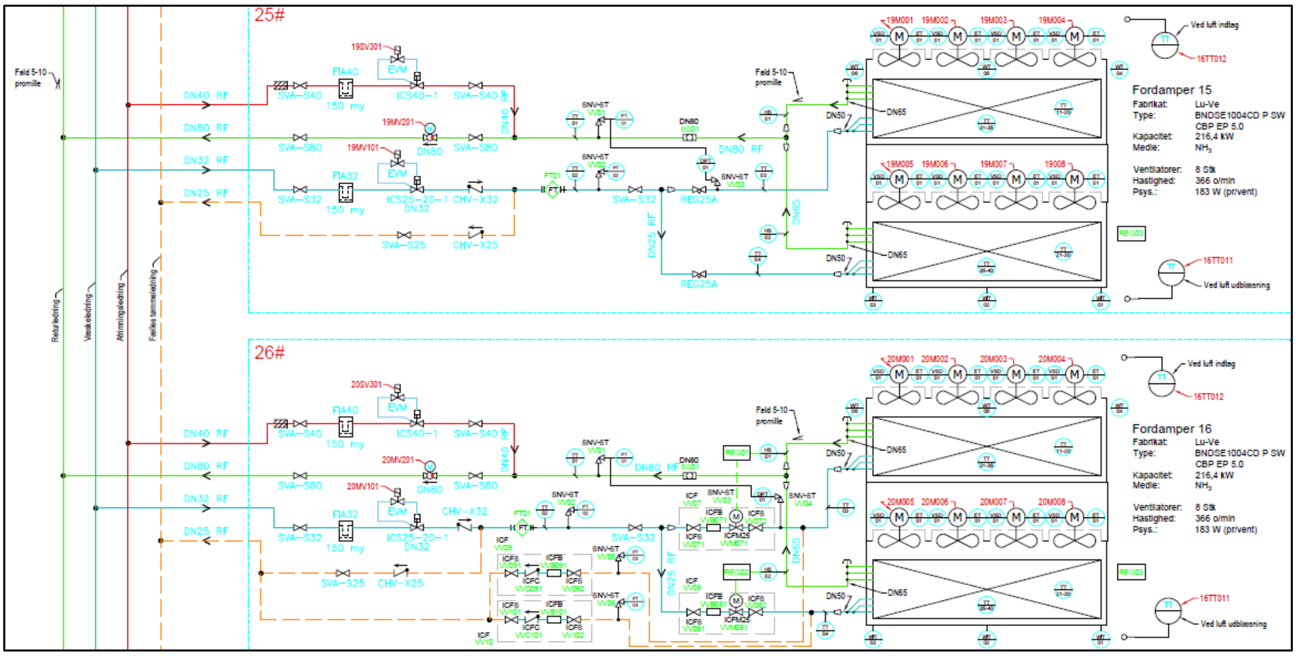

Figure 7: PI-diagram of evaporator #15 and #16 at Brædstrup Fjernvarme

A lot of measurements have been made at evaporators #15 and #16 as shown in figure 8. Temperatures of the air side and the refrigerant side, pressure and pressure difference on the air side and the refrigerant side, relative humidity of the air side, weight of the evaporator, flow on the refrigerant side, rotation speed and direction as well as the absorbed electrical power of each fan. Also weather data has been registered at a weather station, and thermographic photographs and other examinations have been made.

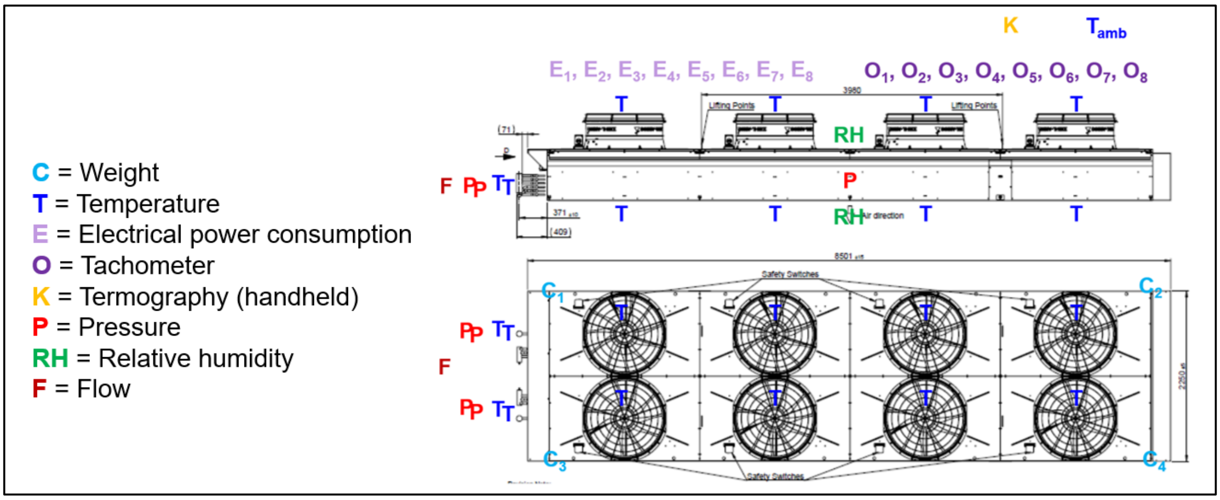

Figure 8: Specification of various measurements on evaporator #16 at Brædstrup Fjernvarme

In the following part of this paper some of the measurements have been selected, commented and analyzed in terms of weather conditions (figure 9), temperatures on the air side (figure 10), the electrical power consumption of each fan (figure 11), evaporation temperatures at headers (figure 12), differential pressure on the refrigerant side (figure 13 as well as weight of the evaporators (figure 14).

3.1. Measurements of weather conditions

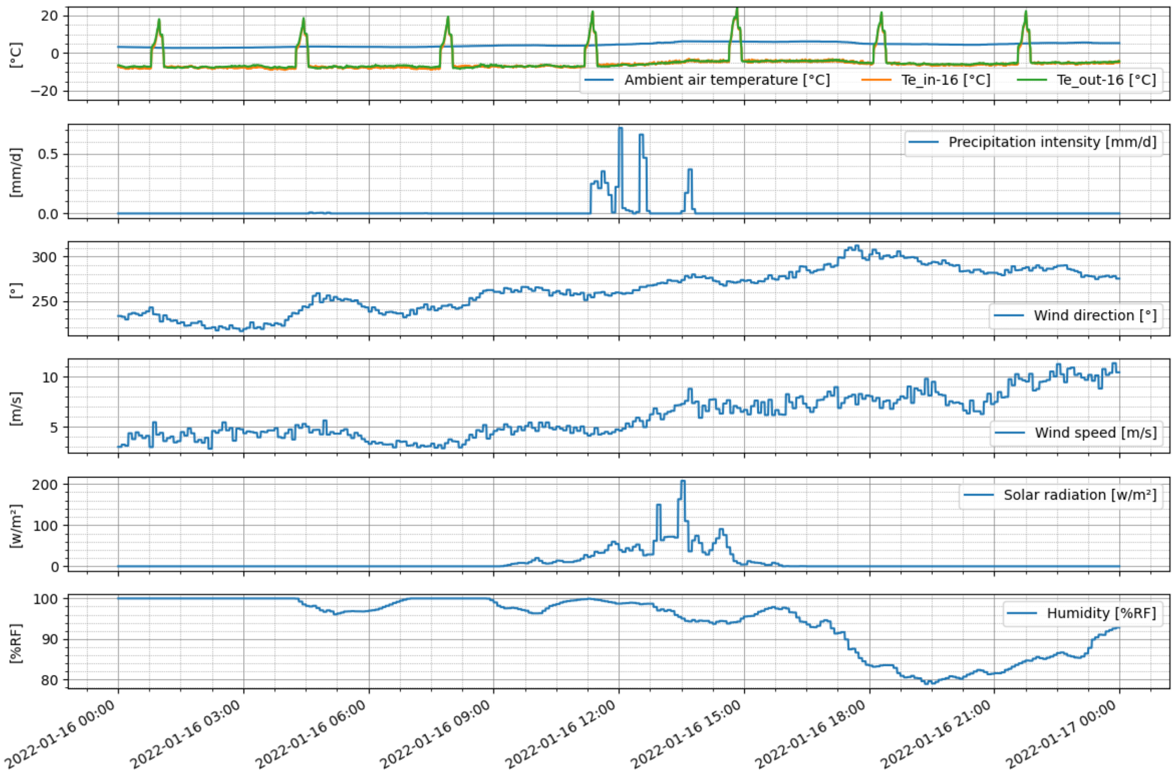

Figure 9: Measurements of weather conditions on top of the accumulation tank at Brædstrup Fjernvarme

Description of measurements:
Ambient air temperature [°C]: The ambient air temperature
Te_in-16: Evaporation temperature at inlet header evaporator (calculated from pressure)
Te_out-16: Evaporation temperature at outlet header evaporator (calculated from pressure)
Precipitation intensity [mm/d]: Precipitation intensity
Wind direction [°]: Wind direction (0°=360°=north)
Wind speed [m/s]: Wind speed
Solar radiation [W/m^2]: Solar radiation
Humidity [%RF]: Relative Humidity

On this specific day, the ambient air temperature varied between approx. +3°C and +6°C. The evaporation temperature varied between approx. -8°C and -4°C. Light rainfall in the middle of the day of up to 1mm/day. Westerly wind direction turning from 220° (southwest) to 310° (northwest). Wind speed was increasing from approx. 3 to approx. 11m/s. Slight solar radiation in the middle of the day up to 200 W/m^2. Humidity was decreasing from approx. 100% to approx. 80%.

Measurements of weather data show a relatively ordinary cold and humid Danish winter day.

3.2. Measurements on the air side

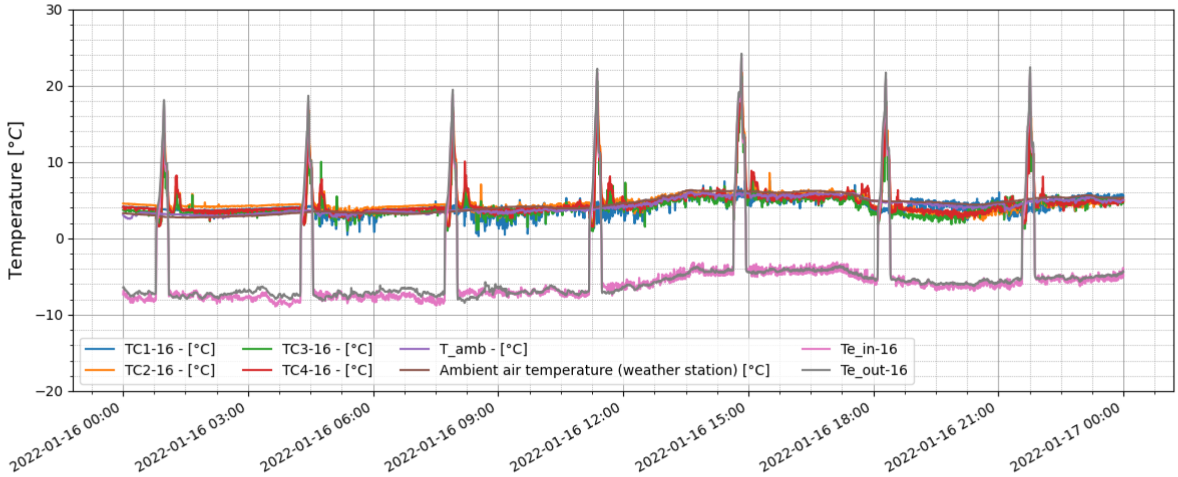

Figure 10: Measurements of the inlet temperatures for the ambient air underneath evaporator #16 at Brædstrup

Description of measurements:
TC1-16, TC2-16, TC3-16, TC4-16: Air temperatures measured underneath evaporator #16 – before cooling
T_amb: Ambient air temperature
Ambient air temperature [°C]: Ambient air temperature
Te_in-16: Evaporation temperature at inlet header evaporator (calculated from pressure)
Te_out-16: Evaporation temperature at outlet header evaporator (calculated from pressure)

The air temperatures underneath the evaporators (inlet) have different patterns during the periods of operation, and they vary much compared to the ambient air temperature with variations of up to 3K. The evaporation temperatures are often between approx. 10 to 12°K below the ambient air temperature.

The temperature measurements show evidence of different degrees of recirculation as predicted by CFD-calculations (Rogié et. all., 2020).

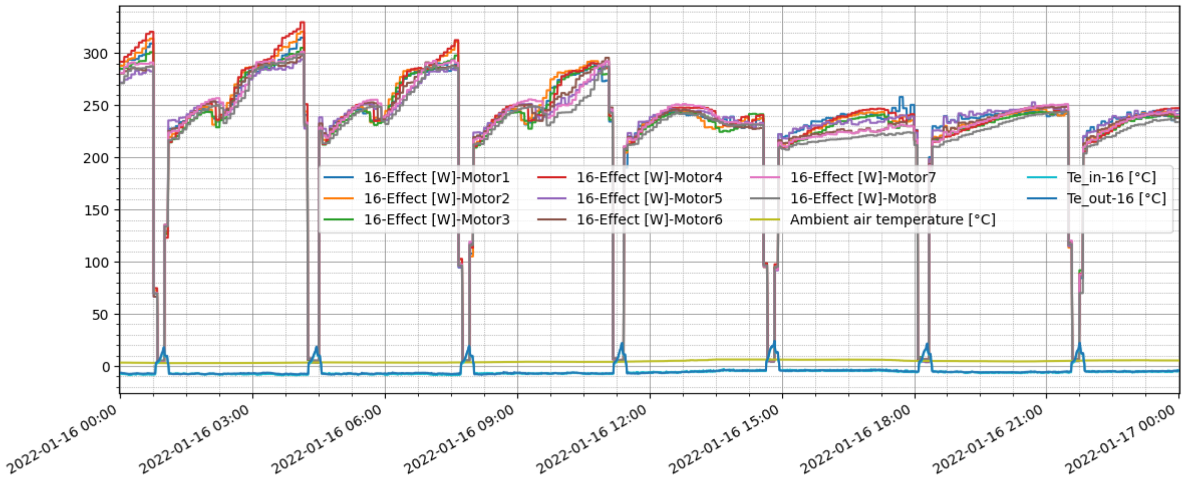

Figure 11: Measurements of electrical power consumption for the eight fans on evaporator #16 at Brædstrup

Description of measurements:
Ambient air temperature [°C]: Ambient air temperature measured by weather station on top of the accumulation tank
16-Effect [W]-Motor1: Electrical power consumption fan 1 on evaporator #16
16- Effect [W]-Motor2: Electrical power consumption fan 2 on evaporator #16

16- Effect [W]-Motor3: Electrical power consumption fan 3 on evaporator #16
16- Effect [W]-Motor4: Electrical power consumption fan 4 on evaporator #16
16- Effect [W]-Motor5: Electrical power consumption fan 5 on evaporator #16
16- Effect [W]-Motor6: Electrical power consumption fan 6 on evaporator #16
16- Effect [W]-Motor7: Electrical power consumption fan 7 on evaporator #16
16- Effect [W]-Motor8: Electrical power consumption fan 8 on evaporator #16
Te_in-16: Evaporation temperature at inlet header evaporator (calculated from pressure)
Te_out-16: Evaporation temperature at outlet header evaporator (calculated from pressure)

The electrical power consumption of the fans starts at almost the same level and increases for each operation period. However, the patterns of each period are very different. The increase is due to frosting, which results in an increased pressure difference in the coil, where there is a significant degree of frosting in the first three periods compared to the last three periods. This change is caused by an increasing temperature and a decreasing relative humidity in the ambient air as well as an incomplete defrosting. In the first three to four periods, a decrease followed by an increase occurs – probably due to stalling of the fans at a specific spot on the performance curve for the fan. Some of the operation periods show that the amount of electrical power consumption is different for each fan. This indicates unequal frosting of each fan's part of the coil or that the tip of the fan blades hit ice in the surrounding pipes.

Measurements of the electrical power consumption of the fans show a large variation dependent on an unequal pressure difference in parts of the coil which in turn depends on the degree of frosting due to the ambient air temperature and relative humidity as well as the stalling of the fans and the fan blades which hit ice in the surrounding "pipe".

3.3. Measurements on the refrigerant side

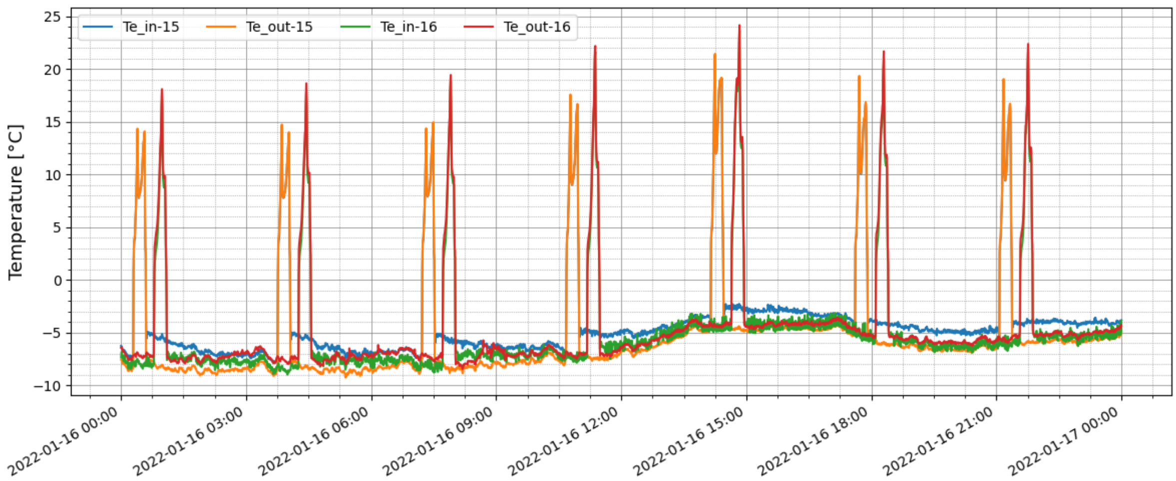

Figure 12: Measurements of evaporation temperatures at inlet and outlet headers on evaporator #15 and #16 at Brædstrup

Description of measurements:
Te_in-15: Evaporation temperature at inlet header evaporator (calculated from pressure)
Te_out-15: Evaporation temperature at outlet header evaporator (calculated from pressure)
Te_in-16: Evaporation temperature at inlet header evaporator (calculated from pressure)
Te_out-16: Evaporation temperature at outlet header evaporator (calculated from pressure)

The evaporation temperatures in the outlet headers (orange and red) for evaporator #15 and #16 should be the same as they are connected to the same pump separator. However, a difference of 1-2^{o}K is registered, which is assumed to be caused by different pressure losses between the headers and the common wet return. The difference in evaporation temperature between inlet and outlet headers is reduced during the operation periods from approx. 1-3°K through evaporator #15 and 0-1°K through evaporator #16. This means that there is a temperature glide from inlet to outlet of the evaporator coils during operation which has a negative effect on the performance of the evaporators. The pressure loss is caused by a decreasing flow of gaseous ammonia through the evaporator coils due to frosting – largest impact at a circulation rate of 2 and least impact at a circulation rate of 1.

The measurements of evaporation temperatures in evaporator #15 and #16 have registered a difference caused by a pressure loss between the headers and the common wet return as well as a temperature glide of up to 3°K during operation periods due to frosting – largest glide at the highest circulation rate – which reduces the performance of the evaporator.

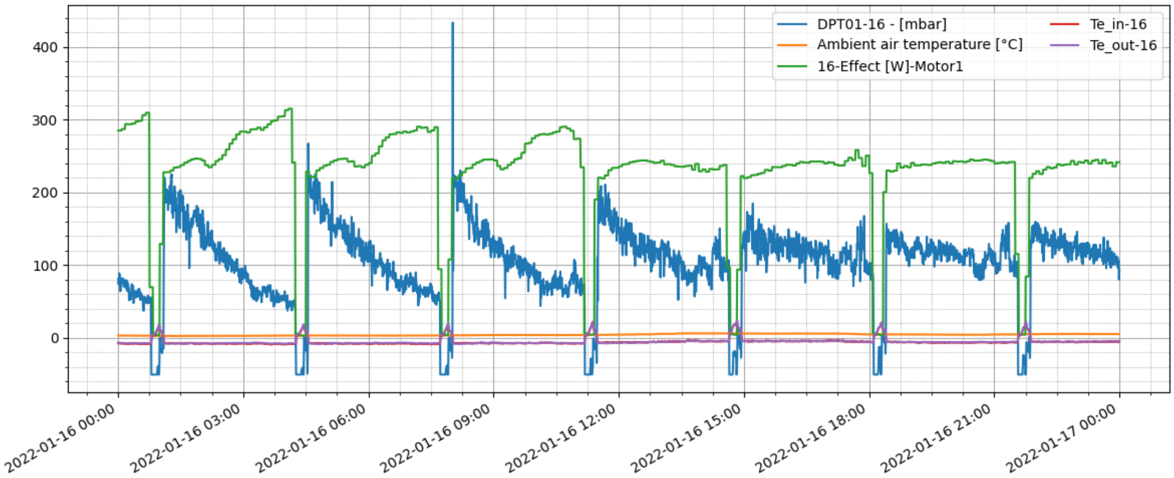

Figure 13: Measurements of differential pressure between inlet and outlet tubes on the ammonia side for evaporator #16 at Brædstrup

Description of measurements:
DPT01-16 – [bar]: Differential pressure on ammonia side between common inlet and outlet pipes for evaporator #16
Ambient air temperature [°C]: Ambient air temperature
16-Effect [W]-Motor1: Absorbed electrical power fan 1 on evaporator #16
Te_in-16: Evaporation temperature at inlet header evaporator (calculated from pressure)
Te_out-16: Evaporation temperature at outlet header evaporator (calculated from pressure)

The measurements of the differential pressure between the common inlet and outlet tubes of the ammonia for evaporator #16 show a decrease during periods of operation with frosting but remains almost at the same level during periods where the evaporator is not completely defrosted.

3.4. Weight measurements

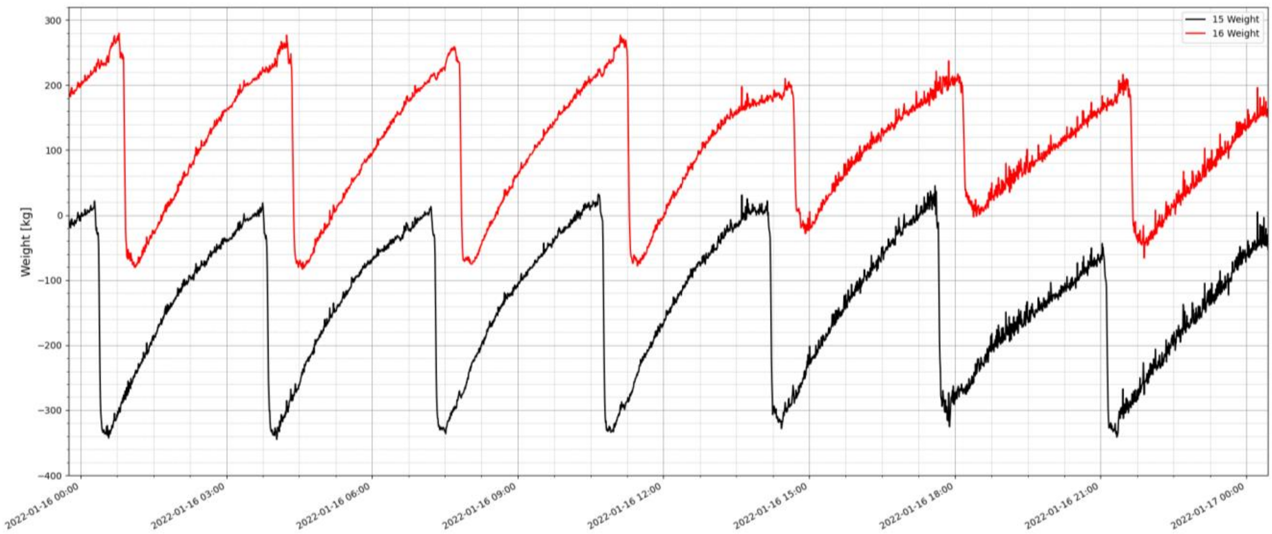

Figure 14: Weight measurements of evaporator #15 and #16 at Brædstrup

Description of measurements:
15 Weight: Weight of evaporator #15
16 Weight: Weight of evaporator #16

The weight increases during operation and decreases during defrosting almost in the same way for both evaporators. The weight increases approx. 200-350 kg during periods of operation. The weight of evaporator #16 does not always reach the minimum level after defrosting, which indicates that the defrosting is incomplete or that the ice has not 'fallen off' for various reasons as observed in several cases.

The weight measurements show that the weight of the evaporators increases by approx. 200-350 kg during operation due to frosting and decreases correspondingly during defrosting. The weight patterns can reveal incomplete defrosting or other reasons for the lack of weight loss during defrosting.

4. RESULTS

The purpose of the measurements was to analyze the data and use the knowledge to optimize and develop the evaporator design and the control for frosting and defrosting through mapping and understanding how this plant works.

4.1. Evaporator performance

In addition to the importance of the design and construction of the evaporators, there are several factors that affect the performance of the evaporators. Of largest importance is the degree of recirculation (see reference), upward or downward air direction as well as the chosen liquid supply system.
The design and construction of the evaporator with regards to performance are i.e., about the configuration of the coil with several parallel passes, pipe dimensions, fin design and spacing as well as design of headers. The evaporators at Brædstrup Fjernvarme are constructed by Luve with two coils in parallel, 5/8" stainless steel pipes in rows of 22 pipes coupled with six headers, and 0.25mm louvered fins with a spacing of 5 mm.

During the project, changes have been made with regards to construction and application of the evaporators. A tightening between the coils and the casing has been made to avoid bypass of ambient air, another coupling of the headers has been made to increase the velocity in the pipes, and the direction of the air flow has been changed from downward to upward to create a homogenic air flow. At the time of writing, the effect of these change has not been analyzed.

CDF calculations (Rogié et. all., 2020) show that a relatively large degree of recirculation can occur at certain 'unfortunate' wind directions, and temperature measurements of ambient air before and after the passage of the evaporators have confirmed this. Unfortunately, the significance of the recirculation for the overall performance of the plant from the twenty evaporators is unknown, but work is under way to be able to calculate this.

Downward flow of ambient air through the evaporator is advantageous to lead water from melted frost and ice by defrosting downwards. The heating of ambient air from supplied electrical energy to the fans will affect the performance positively. Cooled air will try to stay close to the ground surface. A fan which pushes air through a coil will create an uneven air flow through the associated face-area.
Upward flow of the ambient air through the evaporator is advantageous to give a more even air flow through the face-area of the coil as the fan draws the air through the coil. The cooled air will seek towards the ground surface and create recirculation at low wind speeds. In certain situations, e.g., rainfall, the cooled air can contribute to ice formation on the fan blades and surrounding diffusor so that the tip of the fan blades hits ice, which makes noise and increases the electrical power absorption.

Different designs of liquid supply systems cause different degrees of circulation on the ammonia side. The increasing degree of circulation results in an increasing pressure loss with consequent temperature glide through the coil which affects the evaporator performance negatively.

4.2. Defrosting

The plant at Brædstrup Fjernvarme use hotgas for defrosting. The control of the hotgas defrosting is designed in the same way as controls used for large industrial refrigeration and freezing plants with fixed intervals between defrosting sessions and a predetermined duration of defrosting (egg timer method). Measurements and observations show that the intervals between defrosting sessions were either too short or too long depending on the weather conditions. The measurements also show that the duration of the defrosting sessions was either too short leaving the defrosting incomplete or too long resulting in unnecessary energy consumption. Thus, there is a need to develop a more intelligent defrost control that ensures efficient defrosting with minimal energy consumption.

Analyses of the measurements indicate that an intelligent defrost control can be established in terms of appropriate data processing of different measurements to use these signals to start and stop defrosting.

Start signals for defrosting: A signal to start the need for defrosting of an evaporator can be created from intelligent processing of data that detects the build-up of frost/ice. Such a signal could be <u>weight</u>, visual or capacitive registration of ice/frost, <u>differential pressure on the air side</u>, <u>differential pressure on the refrigerant side</u>, temperatures and temperature differences between air inlet and outlet, <u>temperatures on and between fins</u> as well as <u>electrical power consumption for fans</u>. At the time of writing, using data from the underlined options is the most preferred options.

Stop signals for defrosting: A signal to stop a current defrost of an evaporator can be created from intelligent processing of data that detects the removal of frost/ice. Such a signal could be <u>weight</u>, visual or capacitive registration of ice/frost, <u>temperatures on or between fins</u>. At the time of writing, using data from the underlined options is the most preferred options.

At the time of writing, the thoughts and ideas for the new intelligent defrost control have been described and developed. At the time of the conference, the work and test of a new intelligent defrost control will hopefully have progressed substantially.

5. CONCLUSIONS

In an ongoing project, in-depth measurements have been and will be made in the future on 2 out of 20 evaporators installed on a 6.5 MW heat pump system at Brædstrup Fjernvarme. The measurements are made to map and understand exactly how this plant works – and to use this knowledge for optimization and development.

The temperature measurements show signs of different degrees of recirculation.

The measurements of the electrical power consumption of the fans show much variation depending on the unequal pressure difference in parts of the coil which again depends on the degree of defrost due to the ambient air and the relative humidity as well as the stalling of the fans and the fan blades hitting ice in the surrounding “pipe”.

The measurements of the evaporation temperatures in evaporator #15 and #16 have registered a difference due to a pressure drop between headers and the common wet return as well as a temperature glide of up to 3°K through operating periods with frosting – largest impact at the highest circulation rate – wich reduces the performance of the evaporators.

The measurements of the differential pressure between the common inlet and outlet of the ammonia for evaporator #16 show a decrease during operation periods with frosting, but maintain almost the same level during operation periods where the evaporator is not completely defrosted.

The weight measurements show that the weight of the evaporators increases by approx. 200-350 kg during operation due to frosting and decreases correspondingly during defrosting. The weight patterns can reveal incomplete defrosting or other reasons for the lack of weight loss during defrosting.

In addition to the importance of the design and construction of the evaporators, there are several factors that affect the performance of the evaporators. Of most importance is the degree of recirculation, upward or downward air direction as well as the chosen liquid supply system.

Analyses of the measurements indicate that an intelligent defrost control can be established by appropriate processing of data from various measurements in order to use these signals to start and stop defrosting.
There are still registered conditions which at present are not fully understood or explained but work on these matters continues until the planned end of the project in December 2022. It is also the hope that a new intelligent defrost control has been fully developed and tested before the projects ends.

6. ACKNOWLEDGEMENT

Thanks to Danish Energy Technology Development and Demonstration Program (EUDP) who has supported the project financially.

7. REFERENCES

Rogié, B., Jensen, J. K., Hansen, S. O. K., & Markussen, W. B. (2020). Analysis of cold air recirculation in the evaporators of large-scale air-source heat pumps using CFD simulations. *Fluids*, *5*(4), [186].

Jensen, T. G., & Jespersen, E. L. (2019). Potentials and limitations for using ambient air as heat source for large-scale heat pumps

Kristófersson, J., Reinholdt, L., Vestergaard, N., Skovrup, M. J., Wronski, J., & Pachai, A. (2018). Defrost Efficiency for Ammonia Evaporator Systems. Proceedings of the 13th IIR Gustav Lorentzen Conference on Natural Refrigerants. Valencia, Spain: International Institute of Refrigeration.